Published in final edited form as:

*Hepatology*. 2021 July ; 74(1): 164–182. doi:10.1002/hep.31713.

# Mast Cells Promote Nonalcoholic Fatty Liver Disease Phenotypes and Microvesicular Steatosis in Mice Fed a Western Diet

**Lindsey Kennedy**[1], **Vik Meadows**[1], **Amelia Sybenga**[2], **Jennifer Demieville**[3], **Lixian Chen**[1], **Laura Hargrove**[4], **Burcin Ekser**[5], **Wasim Dar**[6], **Ludovica Ceci**[1], **Debjyoti Kundu**[1], **Konstantina Kyritsi**[1], **Linh Pham**[1,#], **Tianhao Zhou**[4], **Shannon Glaser**[4], **Fanyin Meng**[1,7], **Gianfranco Alpini**[1,7], **Heather Francis**[1,7]

[1]Division of Gastroenterology and Hepatology, Department of Medicine, Indiana University School of Medicine, Indianapolis, IN

[2]Department of Pathology, Microbiology, and Immunology, Vanderbilt University School of Medicine, Nashville, TN

[3]Central Texas Veterans Health Care System, Texas A&M University College of Medicine, Bryan, TX

[4]Department of Medical Physiology, Texas A&M University College of Medicine, Bryan, TX

[5]Department of Transplant Surgery, Indiana University School of Medicine, Indianapolis, IN

[6]Division of Immunology and Organ Transplantation, Department of Surgery, University of Texas Health Science Center at Houston, Houston, TX

[7]Richard L. Roudebush VA Medical Center, Indiana University School of Medicine, Indianapolis, IN.

## Abstract

**ADDRESS CORRESPONDENCE AND REPRINT REQUESTS TO:** Heather Francis, Ph.D., F.A.A.S.L.D., Indiana University, Gastroenterology, Medicine, Richard L. Roudebush VA Medical Center, 702 Rotary Circle, Rm. 013C, Indianapolis, IN 46202-2859, heafranc@iu.edu, Tel.: +1-317-278-4222.

[#]Current address: Department of Science & Mathematics, Texas A&M University-Central Texas, Killeen, TX.

*Author Contributions*: L.K. was responsible for conceptualization, data curation, formal analysis, investigation, methodology, validation, visualization, writing–original draft, writing–review, and editing. V.M. was responsible for data curation, formal analysis, investigation, methodology, validation, writing–review, and editing. A.S. was responsible for formal analysis, investigation, validation, writing–review, and editing. L.C. was responsible for data curation, formal analysis, writing–editing. D.K. was responsible for data curation, formal analysis, investigation, methodology, validation, writing–review, and editing. J.D., L.H., L.C., K.K., and L.P. were responsible for data curation, formal analysis, investigation, methodology, and validation. B.E. was responsible for resources. W.D. was responsible for resources and data curation. T.Z. was responsible for software. S.G. was responsible for funding acquisition and resources. F.M. was responsible for writing–review & editing. G.A. was responsible for funding acquisition, resources, writing–review, and editing. H.F. was responsible for conceptualization, formal analysis, funding acquisition, project administration, resources, supervision, visualization, writing–review, and editing.

Potential conflict of interest: Nothing to report.

Supporting Information

Additional Supporting Information may be found at onlinelibrary.wiley.com/doi/10.1002/hep.31713/suppinfo.

The views expressed in this article are those of the authors and do not necessarily represent the views of the Department of Veterans Affairs.

**BACKGROUND AND AIMS:** Nonalcoholic fatty liver disease (NAFLD) is simple steatosis but can develop into nonalcoholic steatohepatitis (NASH), characterized by liver inflammation, fibrosis, and microvesicular steatosis. Mast cells (MCs) infiltrate the liver during cholestasis and promote ductular reaction (DR), biliary senescence, and liver fibrosis. We aimed to determine the effects of MC depletion during NAFLD/NASH.

**APPROACH AND RESULTS:** Wild-type (WT) and $Kit^{W\text{-}sh}$ (MC-deficient) mice were fed a control diet (CD) or a Western diet (WD) for 16 weeks; select WT and $Kit^{W\text{-}sh}$ WD mice received tail vein injections of MCs 2 times per week for 2 weeks prior to sacrifice. Human samples were collected from normal, NAFLD, or NASH mice. Cholangiocytes from WT WD mice and human NASH have increased insulin-like growth factor 1 expression that promotes MC migration/activation. Enhanced MC presence was noted in WT WD mice and human NASH, along with increased DR. WT WD mice had significantly increased steatosis, DR/biliary senescence, inflammation, liver fibrosis, and angiogenesis compared to WT CD mice, which was significantly reduced in $Kit^{W\text{-}sh}$ WD mice. Loss of MCs prominently reduced microvesicular steatosis in zone 1 hepatocytes. MC injection promoted WD-induced biliary and liver damage and specifically up-regulated microvesicular steatosis in zone 1 hepatocytes. Aldehyde dehydrogenase 1 family, member A3 (ALDH1A3) expression is reduced in WT WD mice and human NASH but increased in $Kit^{W\text{-}sh}$ WD mice. MicroRNA 144-3 prime (miR-144-3p) expression was increased in WT WD mice and human NASH but reduced in $Kit^{W\text{-}sh}$ WD mice and was found to target ALDH1A3.

**CONCLUSIONS:** MCs promote WD-induced biliary and liver damage and may promote microvesicular steatosis development during NAFLD progression to NASH through miR-144-3p/ALDH1A3 signaling. Inhibition of MC activation may be a therapeutic option for NAFLD/NASH treatment. (HEPATOLOGY 2021;74:164–182).

Nonalcoholic fatty liver disease (NAFLD) can develop into nonalcoholic steatohepatitis (NASH).[1] High mortality rates are seen in patients with NAFLD, and NASH is the third most common indication for liver transplantation in the United States.[2,3] During NAFLD, macrovesicular steatosis is characterized as hepatocytes with a single, large vacuole of fat that displaces the nucleus and is considered benign.[4] Microvesicular steatosis, in NASH, is described as hepatocytes with numerous, small lipid vesicles that do not displace the nucleus, entailing a more severe prognosis.[4,5] Ductular reaction (DR) and biliary senescence are found in patients with NASH, and DR positively correlates with liver fibrosis during NASH.[6,7]

Mast cells (MCs) are key mediators of allergies and inflammation.[8] MC number increases in cholangiopathies, such as primary sclerosing cholangitis (PSC) and cholangiocarcinoma (CCA), and in the bile duct–ligated (BDL) and multidrug resistance 2-knockout ($Mdr2^{-/-}$) mouse models of cholestasis.[9–11] We have demonstrated that (1) MCs reside near injured ducts, (2) MC infiltration is preceded by cholangiocyte proliferation following BDL,[10–12] and (3) inhibition or genetic loss of MCs reduces DR, biliary senescence, and liver fibrosis in BDL and $Mdr2^{-/-}$ mice.[9,10] Serum histamine (released by activated MCs) levels increase in patients with NAFLD or NASH[6]; however, the direct role of MCs is unknown.

MicroRNAs (miRNAs) are dysregulated during NAFLD and can be diagnostic or prognostic markers during disease progression.[13] Hepatic miRNA 144-3 prime (miR-144-3p)

expression increases in patients with NASH[13]; however, another group has found that miR-144-3p is reduced in Kupffer cells (KCs) from rats fed a high-fat diet (HFD).[13] The direct role of miR-144-3p during NAFLD/NASH is controversial.

Aldehyde dehydrogenase 1 family, member A3 (ALDH1A3) detoxifies aldehydes generated by lipid peroxidation.[14] Lipid peroxidation occurs when oxidants attack lipids containing carbon–carbon double bonds, leading to production of malondialdehyde (MDA).[15] Hepatic ALDH1A3 expression is reduced in human NAFLD and NASH,[16] and enhanced lipid peroxidation correlates with hepatic steatosis and liver fibrosis in NASH.[17] Additionally, lipid peroxidation increases microvesicular steatosis, which is accompanied by reduced β-oxidation.[18,19]

We evaluated the role of MCs in the progression of steatosis, DR, biliary senescence, inflammation, liver fibrosis, and angiogenesis in a mouse model of NAFLD using a Western diet (WD; high-fat, trans-fat with high cholesterol and high-fructose corn syrup equivalent) feeding model. Our data indicate a role for MCs in the induction of WD-induced phenotypes including microvesicular steatosis through miR-144-3p/ALDH1A3 signaling.

## Materials and Methods

### MATERIALS

Total RNA was isolated from liver tissues, selected cell lines, and isolated cholangiocytes and hepatocytes using TRI Reagent. miRNA was isolated from liver tissues and isolated hepatocytes using the mirVana miRNA Isolation Kit (Ambion, Mountain View, CA). mRNA was reverse-transcribed with the iScript cDNA synthesis kit (Bio-Rad, Hercules, CA). Primers were purchased from Qiagen (Valencia, CA) and are described in Supporting Table S1. Quantitative PCR was performed using the $RT^2$ SYBR Green/ROX quantitative PCR master mix for the Applied Biosystems ViiA7 quantitative PCR system (Life Technologies, Carlsbad, CA). For mouse and human staining, formalin-fixed, paraffin-embedded samples were sectioned at 4–6 μm; optimal cutting temperature–embedded sections were sectioned at 6–8 μm; at least 10 fields were analyzed. Antibodies are described in Supporting Table S2. All other reagents, chemicals, and cell culture details are provided in the Supporting Information.

### ANIMAL MODELS

Animal procedures were performed according to protocols approved by the Baylor Scott & White Health and Indiana University School of Medicine (IUSM) institutional animal care and use committees. MC-deficient mice (B6.Cg-*Kit*$^{W\text{-}sh}$/HNihrJaeBsmJ, i.e., *Kit*$^{W\text{-}sh}$) and background-matched wild-type (WT; C57BL/6J) were purchased from Jackson Laboratory (Bar Harbor, ME). Animals were housed in microisolator cages in a temperature-controlled environment with 12:12 hour light–dark cycles. Studies were performed in 4-week-old male WT and *Kit*$^{W\text{-}sh}$ mice fed a control diet (CD) consisting of standard chow and reverse-osmosis water or the WD consisting of a high-fat trans-fat diet (45% calories from fat and 0.2% cholesterol; Envigo, Indianapolis, IN) coupled with 55% fructose and 45% glucose w/w dissolved in reverse-osmosis water for 16 weeks, which induces steatosis,

inflammation, and fibrosis in normal mice.[6] Selected WT WD and *Kit*$^{W\text{-}sh}$ WD mice received tail vein injections of $5 \times 10^6$ tagged (PKH26 Red Fluorescent Cell Linker), cultured MCs (MC/9; ATCC, CRL-8306) suspended in 0.1 mL of 1× phosphate-buffered saline (PBS) or 0.1 mL 1× PBS 2 times per week for 2 weeks following 14 weeks of feeding. Animal numbers for each group were as follows: WT CD, n = 15 mice; WT WD, n = 10 mice; *Kit*$^{W\text{-}sh}$ CD, n = 8 mice; *Kit*$^{W\text{-}sh}$ WD, n = 13 mice; WT WD+MC, n = 13 mice; and *Kit*$^{W\text{-}sh}$ WD+MC, n = 11 mice. Liver tissues, serum, hepatocytes, and cholangiocytes were collected.[6,9] Cholangiocytes were isolated using a monoclonal antibody (IgM; a gift from Dr. Ronald A. Faris, Brown University, Providence, RI).[10]

### HUMAN SAMPLES

Human liver tissues were collected from patients diagnosed with NAFLD or NASH and nondiseased controls by Dr. Wasim Dar at the University of Texas Health Science Center and Dr. Burcin Ekser at IUSM or purchased from Sekisui XenoTech, LLC (Kansas City, KS); these samples were used for RNA extraction, protein extraction, and liver sections for staining. Explant tissues were obtained from transplant, and the diagnosis of NAFLD or NASH was determined by clinical, imaging, and pathological analyses. Written informed consent was obtained from each patient, and the study protocol conformed to the ethical guidelines of the 1975 Declaration of Helsinki as reflected in *a priori* approval by the University of Texas Health Science Center and Indiana University institutional review boards (no donor organs were obtained from executed prisoners or other institutionalized persons). Samples were deidentified, and patient information is provided in Supporting Table S3. All other experimental procedures are detailed in the Supporting Information.

### STATISTICAL ANALYSIS

Data are expressed as the mean ± SEM. Differences between groups were analyzed by the Student unpaired *t* test when two groups were analyzed and by two-way ANOVA when more than two groups were analyzed.

## Results

### BILIARY INSULIN-LIKE GROWTH FACTOR-1 DRIVES MC MIGRATION, AND MC INFILTRATION/ACTIVATION INCREASES DURING NAFLD/NASH

We first evaluated changes in cytokine release from cholangiocytes isolated from WT CD and WT WD mice to determine potential MC chemoattractant candidates. We found that several interleukins and growth factors along with leptin and resistin increased in cholangiocyte supernatants from WT WD mice compared to WT CD mice (Fig. 1A), and the fold change of insulin-like growth factor-1 (IGF-1) secretion had the highest change (Fig. 1B). Hepatic IgE levels, a key mediator of MC histamine release, increased in WT WD mice compared to WT CD mice (Fig. 1C); however, IgE release from cholangiocytes was not detected (data not shown). To evaluate cholangiocyte-derived factors, we verified our multiELISA findings by increased IGF-1 secretion in cholangiocyte supernatants and serum (Fig. 1D) and expression in liver sections (Fig. 1E) in WT WD mice compared to WT CD mice. We found no change in hepatocyte IGF-1 secretion between WT CD and WT WD mice (data not shown). Notably, MCs have been shown to express and be activated

by IGF-1.[20] In human samples, we found an increase in biliary IGF-1 immunoreactivity in those with NASH compared to controls (Fig. 1F). Lastly, *in vitro*, we verified that inhibition of IGF-1 receptor (IGF-1R) blocks MC migration. We found that free fatty acid (FFA)–treated cholangiocyte supernatants induce MC migration, which is blocked following treatment with the IGF-1R inhibitors AG 583, linsitinib, and picropodophyllin (Supporting Fig. S1)

In WT WD mice, MC (red arrows) numbers increased compared to WT CD mice and were found primarily surrounding bile ducts[10–12] as shown by mouse MC protease 1 (mMCP-1) staining (Fig. 2A). Furthermore, hepatic expression of chymase, tryptase, and KIT proto-oncogene receptor tyrosine kinase (c-Kit; MC-specific markers; Fig. 2B) and serum histamine levels (Fig. 2C) increased in WT WD mice compared to WT CD mice.

MC presence (tryptase, red) slightly increased in NAFLD and increased in NASH compared to control samples; increased MC presence corresponded with enhanced DR (cytokeratin 19 [CK-19], brown), and MCs were found surrounding bile ducts (Fig. 2D). These findings were supported by increased MC marker expression in NASH, with a trend toward increasing in NAFLD, compared to control (Fig. 2E).

## MC DEPLETION DECREASES WD-INDUCED LIVER DAMAGE AND STEATOSIS

We determined the role of MCs in WD-induced damage by feeding WT or $Kit^{W\text{-}sh}$ mice the CD or WD for 16 weeks (Supporting Fig. S2A). Macroscopic images showed that livers of WT WD mice were pale compared to those of WT CD mice; no significant color changes were noted in $Kit^{W\text{-}sh}$ CD or WD mice (Supporting Fig. S2B). Overall, WT WD mice had increased liver weight (LW) and LW/body weight (BW) ratio compared to WT CD mice, which was reduced in $Kit^{W\text{-}sh}$ WD mice compared to WT CD mice; no changes were noted in BW between all groups (Supporting Fig. S2C). Hematoxylin and eosin (H&E) staining showed that WT WD mice have >95% of hepatocyte involvement in macrovesicular and microvesicular steatosis in zone 1 and zone 2, with small lymphocytic aggregates, and were diagnosed with severe steatosis (Fig. 3A). $Kit^{W\text{-}sh}$ WD mice presented with 50%−70% hepatocytes involved in steatosis, with macrovesicular steatosis found in zone 1 and microvesicular steatosis found in zone 2, with no increase in inflammation, and were diagnosed with moderate steatosis (Fig. 3A). Serum levels of alanine aminotransferase (ALT) increased in WT WD mice compared to WT CD mice but were reduced in $Kit^{W\text{-}sh}$ WD mice compared to WT WD mice (Fig. 3B). Importantly, MC depletion decreased microvesicular steatosis in zone 1, which lies adjacent to the portal triad, in WT WD mice.

Oil red O staining and semiquantification showed increased hepatic steatosis in WT WD mice compared to WT CD mice; however, $Kit^{W\text{-}sh}$ WD mice had reduced hepatic steatosis compared to WT WD mice (Fig. 3C). Similarly, hepatic triglyceride (TG) levels increased in WT WD mice compared to WT CD mice but decreased in $Kit^{W\text{-}sh}$ WD mice compared to WT WD mice (Fig. 3C). Hepatocyte expression of lipogenesis markers increased in WT WD mice compared to WT CD mice but decreased in $Kit^{W\text{-}sh}$ WD mice compared to WT CD mice (Fig. 3D). Conversely, β-oxidation markers decreased in WT WD mice compared to WT CD mice, whereas $Kit^{W\text{-}sh}$ WD mice had increased expression of β-oxidation markers compared to WT WD mice (Fig. 3D).

## WD-INDUCED DR AND BILIARY SENESCENCE DECREASED IN MC-DEFICIENT MICE

We found increased DR (Fig. 4A) and biliary proliferation (Fig. 4B) in WT WD mice compared to WT CD mice, which were reduced in *Kit*$^{W\text{-}sh}$ WD mice compared to WT WD mice. Aside from DR, biliary senescence is enhanced in patients with NAFLD or NASH,[6] and we found increased biliary senescence in WT WD mice compared to WT CD mice shown by p16, senescence-associated β-galactosidase (SA-β-Gal) staining, and mRNA expression of senescence markers in isolated cholangiocytes; however, *Kit*$^{W\text{-}sh}$ WD mice had decreased biliary senescence compared to WT WD mice (Fig. 4C–E). MCs promote DR and mediate biliary senescence during NAFLD, which is also supported by our previous work.[6]

## WD-INDUCED INFLAMMATION, HEPATIC FIBROSIS, AND HEPATIC STELLATE CELL NUMBER ARE REDUCED IN MC-DEFICIENT MICE

Inflammation is key for NAFLD–NASH transition, and we found increased KC presence in WT WD mice compared to WT CD mice; however, *Kit*$^{W\text{-}sh}$ WD mice had decreased KC presence compared to WT WD mice (Fig. 5A). Similar findings were shown for C-C motif ligand 3 (CCL3), CCL4, and CCL5 expression (Fig. 5B) and IL-6 immunostaining (Fig. 5C).

MC activation promotes liver fibrosis during cholestasis,[10,11] and WT WD mice had increased collagen deposition, collagen type 1 α1 (Col1a1) expression, and hydroxyproline content compared to WT CD mice; however, these findings were reduced in *Kit*$^{W\text{-}sh}$ WD mice compared to WT WD mice (Fig. 5D,E). Similarly, hepatic stellate cell (HSC) presence increased in WT WD mice compared to WT CD mice, as shown by desmin staining, but was markedly reduced in *Kit*$^{W\text{-}sh}$ WD mice compared to WT WD mice (Fig. 5F)

## WD-INDUCED VASCULAR ENDOTHELIAL GROWTH FACTOR A EXPRESSION AND ANGIOGENESIS ARE DECREASED IN MC-DEFICIENT MICE

Previous work has shown that MC activation promotes angiogenesis and vascular endothelial growth factor A (VEGF-A) levels during cholestasis.[9,21] We found that hepatic VEGF-A expression increased in total liver and isolated cholangiocytes in WT WD mice compared to WT CD mice; however, VEGF-A gene expression (Supporting Fig. S3A) and immunoreactivity (Supporting Fig. S3B) decreased in *Kit*$^{W\text{-}sh}$ WD mice compared to WT WD mice. Additionally, patients with NAFLD or NASH had increased expression of VEGF-A (brown), along with increased MC presence (red), compared to controls (Supporting Fig. S3C).

WT WD mice had increased angiogenesis compared to WT CD mice, as demonstrated by von Willebrand factor (vWF) staining; however, *Kit*$^{W\text{-}sh}$ WD mice had reduced angiogenesis compared to WT WD mice (Supporting Fig. S3D). Importantly, vWF expression increased in patients with NAFLD and NASH compared to controls (Supporting Fig. S3E), demonstrating that angiogenesis contributes to NAFLD/NASH.

## LOSS OF MCS REVERSES miR-144-3P TARGETING OF ALDH1A3 AND SUBSEQUENT LIPID PEROXIDATION

We found that MC loss primarily reduces zone 1 microvesicular steatosis (Fig. 3A). The presence of microvesicular steatosis indicates a worsening phenotype and is generally associated with impaired β-oxidation, oxidative stress, and toxin clearance.[5] Suppression of ALDH1A3 has been noted in patients with NAFLD[16]; therefore, we postulated that MCs mediate microvesicular steatosis through ALDH1A3 dysregulation. We found that, in WT WD mice, there is increased MC presence (white arrows) corresponding with reduced ALDH1A3 expression when compared to WT CD mice; however, ALDH1A3 expression is restored in *Kit*$^{W\text{-}sh}$ WD mice compared to WT WD mice, shown by immunostaining and western blotting in isolated hepatocytes (Fig. 6A). In human NASH samples there is reduced ALDH1A3 expression compared to controls, determined by immunostaining and western blotting in total liver (Fig. 6B). No changes in the mRNA expression of ALDH1A3 were found in our mouse models or human samples (Supporting Fig. S4A,B), indicating posttranscriptional regulation.

Because we hypothesize that posttranscriptional modifications mediate ALDH1A3 suppression, we used TargetScan software to screen for various miRNA targets and found that miR-144-3P was a highly conserved target for both mouse and human ALDH1A3 sequence (Fig. 6C). miR-144-3P targeting of ALDH1A3 was verified by Ingenuity Pathway Analysis (IPA; Fig. 6C). We found that miR-144-3P expression significantly increased in total liver and isolated hepatocytes from WT WD mice compared to WT CD mice; however, miR-144-3P expression decreased in *Kit*$^{W\text{-}sh}$ WD mice compared to WT WD mice (Fig. 6D). In human samples, miR-144-3P levels were significantly increased in total liver from patients with NASH compared to controls (Fig. 6E). Lastly, by luciferase assay we determined that miR-144-3P targets and decreases the expression of Aldh1a3, but no targeting occurred in the mutated form of Aldh1a3 (Fig. 6F).

ALDH1A3 down-regulation is associated with lipid peroxidation,[22] which can be a driver of microvesicular steatosis[23]; and we found that hepatic MDA levels significantly increased in WT WD mice compared to WT CD mice but significantly decreased in *Kit*$^{W\text{-}sh}$ WD mice compared to WT WD mice (Supporting Fig. S4C).

## MC INJECTION PROMOTES LIVER DAMAGE AND MICROVESICULAR STEATOSIS DURING WD FEEDING

To demonstrate that MCs mediate WD-induced changes, we reintroduced MCs during the last 2 weeks of feeding (Supporting Fig. S5A). Macroscopic liver images and LW/BW ratios are provided (Supporting Fig. S5B,C), and injected MCs (red) are found surrounding bile ducts (Supporting Fig. S5D).

H&E staining demonstrated that WT WD+MC mice presented with 30%−90% steatosis, predominantly microvesicular steatosis, ranging from zone 1 to zone 2. Interestingly, there was more microvesicular, and less macrovesicular, steatosis in WT WD+MC mice compared to WD alone (Fig. 7A), indicating a switch in steatotic phenotype. WT WD+MC mice had rare foci of inflammation and increased duct profiles in portal areas (not seen in WD alone)

and were diagnosed with mild steatohepatitis (Fig. 7A). MC injection into *Kit*$^{W\text{-}sh}$ WD mice (which presented with macrovesicular steatosis in zone 1 and microvesicular steatosis in zone 2 in mice without MC injection) demonstrated microvesicular steatosis in zones 1 and 2 (Fig. 7A). *Kit*$^{W\text{-}sh}$ WD+MC mice had mild DR and few foci of lobular inflammation, which was not present in WD alone, and were diagnosed with mild steatohepatitis (Fig. 7A). MC injection promotes microvesicular steatosis development, particularly in zone 1 hepatocytes, which may be due to MC honing to portal areas.

MC injection into WT WD and *Kit*$^{W\text{-}sh}$ WD mice increased ALT levels compared to WD alone (Fig. 7B). We have previously found that MC injection into normal *Kit*$^{W\text{-}sh}$ mice does not increase serum aspartate aminotransferase (AST) and ALT[9]; therefore, MCs may exacerbate damage when an insult has already occurred.

Unexpectedly, lipid deposition was reduced in WT WD+MC mice compared to WT WD alone, which may indicate a worsening phenotype considering a loss of steatosis quantity in lieu of inflammation and fibrosis can be seen in the NAFLD to NASH transition[5]; however, MC injections increased lipid deposition in *Kit*$^{W\text{-}sh}$ WD mice compared to WD alone (Fig. 7C). Increased lipid droplet area may occur in *Kit*$^{W\text{-}sh}$ WD mice but not WT WD mice because they previously did not have the same degree of WD-induced macrovesicular steatosis (Fig. 3A,C). Therefore, H&E staining demonstrates a switch from primarily macrovesicular to microvesicular steatosis, which may explain less lipid deposition in WT WD+MC mice. Similarly, hepatic TG levels were unchanged in WT WD+MC mice but significantly increased in *Kit*$^{W\text{-}sh}$ WD+MC mice compared to WD alone (Fig. 7C).

## MC INJECTION PROMOTES WD-INDUCED BILIARY AND LIVER DAMAGE VIA THE MIR-144-3P/ALDH1A3 AXIS

DR (Supporting Fig. S6A), biliary senescence (Supporting Fig. S6B), and inflammation (Supporting Fig. S6C) increased in both WT WD and *Kit*$^{W\text{-}sh}$ WD mice following MC injection compared to WD alone. Similarly, MC injection increased liver fibrosis and HSC presence in WT WD and *Kit*$^{W\text{-}sh}$ WD mice compared to WD alone (Supporting Fig. S7A,B). There was a larger degree of liver fibrosis in WT WD mice injected with MCs than *Kit*$^{W\text{-}sh}$ WD mice, which may be due to preexisting liver damage.

MC injection into WT and *Kit*$^{W\text{-}sh}$ WD mice increased VEGF-A expression (Supporting Fig. S8A) and angiogenesis (Supporting Fig. S8B) compared to WD alone. Hepatic miR-144-3p expression increased, while ALDH1A3 expression decreased, and MDA levels increased in WT WD and *Kit*$^{W\text{-}sh}$ WD mice following MC injections (Supporting Fig. S8C–E). These findings confirm that MCs promote WD-induced biliary and liver damage and may correspond with worsening phenotypes.

## IN VITRO, FFAS PROMOTE BILIARY SENESCENCE, AND INJURED CHOLANGIOCYTES, BUT NOT HEPATOCYTES, DRIVE MC MIGRATION

FFAs increase senescence and angiogenesis markers in cultured cholangiocytes compared to basal (BS) (Supporting Fig. S9A). Pooled cultured cholangiocytes, but not hepatocytes, pretreated with FFAs increased MC migration compared to BS (Supporting Fig. S9B), which corresponds with our hypothesis that cholangiocyte-derived IGF-1 promotes MC migration.

Furthermore, these *in vitro* findings confirm that MCs are drawn to injured cholangiocytes, but not hepatocytes, explaining why MCs are found near portal triads.

### IN VITRO, MC-DERIVED HISTAMINE PROMOTES BILIARY SENESCENCE, HEPATOCYTE STEATOSIS, AND ACTIVATION OF KCS AND HSCS

*In vitro*, we treated MCs with compound 48/80 (to induce MC release of histamine) and found that histamine release significantly increased compared to MC BS (Supporting Fig. S10A). *In vitro*, Pool+MC treatments increased SA-β-Gal activity compared to BS treatment, and Pool+MC-48/80 treatments (containing increased histamine levels) had a further increase in SA-β-Gal activity compared to Pool+MC (Supporting Fig. S10B). Cultured mouse hepatocytes were treated with FFAs, along with MC or MC-48/80 supernatants, to evaluate lipogenesis. Following FFA treatments, mouse hepatocytes had increased lipid droplet area, which was further enhanced when FFA treatment was combined with MC supernatants (Supporting Fig. S10C). Interestingly, mouse hepatocytes treated with FFAs and MC-48/80 supernatants had further increased lipid droplet deposition compared with FFA+MC treatments (Supporting Fig. S10C), highlighting the potential role for MC-derived histamine in the promotion of hepatocyte lipogenesis. Lastly, cultured mouse KCs (mKC) and mouse HSCs (mHSC) were treated with supernatants from MC or MC-48/80. mKC+MC had increased TNF-α immunoreactivity compared to BS, which was further increased in mKC+MC-48/80 treatments (Supporting Fig. S10D). Similarly, mHSC+MC showed increased α-smooth muscle actin immunoreactivity compared to BS, which was further enhanced in mHSC+MC-48/80 treatments (Supporting Fig. S10E).

## Discussion

MCs contribute to microvesicular steatosis, DR, biliary senescence, inflammation, angiogenesis, and hepatic fibrosis during NAFLD/NASH. MC deficiency reduces WD-induced injuries, and MC injection into WT and MC-deficient mice exacerbates damage. We propose that MCs drive worsening phenotypes, including microvesicular steatosis development, through miR-144-3p/ALDH1A3 signaling. Additionally, we found that following WD, biliary IGF-1 expression/secretion enhances and may induce MC infiltration near injured bile ducts. Our overall working model is presented in Fig. 8.

DR (1) correlates with fibrosis staging in patients with NAFLD,[7] (2) promotes oxidative stress in pediatric patients with NAFLD, and (3) correlates with liver fibrosis in patients with NASH.[24] In our model, loss of MCs reduced WD-induced DR, which is promoted following MC injection. To support this finding, mice lacking histamine signaling have reduced DR following WD feeding; however, the impact of MCs or MC-derived histamine was not evaluated in this study.[6] In other reports, MC presence increases in patients and murine models of PSC, and inhibition of MC activation/histamine signaling or genetic loss of MCs reduces DR in these models.[9,21,25] Furthermore, infiltrating MCs are found surrounding bile ducts,[10,11,21] which mirrors the findings in this paper. Both parenchymal and periportal MC concentrations increase in NASH, but total number of MCs and changes in MC infiltration are more prominent in the periportal region.[26] We found that MCs were adjacent to damaged ducts in our mouse model and human samples of NAFLD and NASH,

and *in vitro* FFAs promote MC migration toward cholangiocytes, but not hepatocytes, through IGF-1. Others have found that MCs reside near portal areas in chronic liver diseases and are predominantly found in cholestatic liver injuries.[27] Additionally, it has been shown that IGF-1 promotes MC activation.[20] This supports our hypothesis that injured cholangiocytes interact with MCs to promote migration during NAFLD/NASH. Hepatic IgE levels increased in WT WD mice, which may allude to the role of hepatic plasma cells or B cells in the promotion of MC infiltration and activation; however, cellular crosstalk between MCs and other immune cells requires further investigation.

Previous work found that mice lacking histamine signaling (and that have fewer and morphologically altered MCs) have reduced WD-induced inflammation compared to WT WD mice.[6] In our model, hepatic inflammation decreased in MC-deficient WD mice, which was reactivated following MC injection. Apolipoprotein E–deficient ($ApoE^{-/-}$) mice that were crossed with $Kit^{W\text{-}sh/W\text{-}sh}$ (MC-deficient model) and subjected to HFD feeding had reduced IL-6 and IL-10 serum levels compared to $ApoE^{-/-}$ HFD mice,[28] which is important considering that patients with simple steatosis have increased IL-6 serum levels.[29] Furthermore, we found *in vitro* that MC-derived histamine promotes KC activation. One study found that endogenous histamine synthesis in KCs protects from lipopolysaccharide (LPS)–induced hepatitis through activation of the H2 histamine receptor (HR),[30] but others have found that H4HR activation promotes TNF-α synthesis in a rat model of LPS-induced inflammation.[31] Our work has shown that histamine treatment increases KC number and liver inflammation in mice.[32] Overall, the MC and histamine impact on KCs is controversial and may depend on HR expression.

There is a strong link between MC activation and liver fibrosis during cholestasis,[9–11] and hepatic MC concentration correlates with fibrosis in patients with NASH.[26] Previous work found that loss of histamine signaling reduces liver fibrosis during WD feeding,[6] and we found that liver fibrosis and HSC activation were reduced in MC-deficient WD mice but that MC injection exacerbates these parameters. Others have shown that inhibition of chymase (secreted by activated MCs) reduced liver fibrosis in hamsters fed a methionine-deficient and choline-deficient diet,[33] showing that MC inhibition reduces liver fibrosis. We have previously shown that HSCs express H1HR,[10] and inhibition of MC activation blocks HSC activation and liver fibrosis in cholestatic models.[9,21] Furthermore, histamine treatment promotes liver fibrosis and HSC presence[32]; however, the direct impact of histamine on HSCs is undefined and requires further work.

Patients with NAFLD have increased hepatic angiogenesis,[34] and hepatic VEGF-A levels are increased in patients with NASH.[29] Increased angiogenesis and VEGF-A expression are noted in patients with PSC,[35] and, furthermore, MC number corresponds with hepatic VEGF levels and angiogenesis in mouse models of PSC and CCA.[9,10] In MCs isolated from BDL rats, there is increased VEGF-A expression and secretion,[12] showing that hepatic MCs have a proangiogenic phenotype. We found that loss of MCs ameliorates VEGF-A levels and reduces angiogenesis in our NAFLD model. Similarly, previous work has found that loss of histamine synthesis reduces VEGF-A expression and subsequent angiogenesis in a mouse model of PSC.[32]

One key finding of our research was that MCs predominantly modulate microvesicular steatosis development following WD feeding. Microvesicular steatosis is a separate entity from macrovesicular steatosis and correlates with higher grades of steatosis, NAFLD activity scores, fibrosis, and diagnosis of NASH.[5] Patients receiving allografts with >15% microvesicular steatosis have reduced graft survival and higher AST peaks immediately posttransplant.[36] While increased microvesicular steatosis has been identified as a prognostic marker for NAFLD outcomes, the pathogenesis of this development is unknown. We found that MCs promote microvesicular steatosis development, suggesting that MC presence indicates a poor outcome; and others have found that MC density correlates with steatosis, inflammation, and fibrosis in patients with hepatitis C virus.[37] It is unknown if MCs mediate macrovesicular and/or microvesicular steatosis. Interestingly, loss of MCs significantly reduced LW and LW/BW ratios but had no effect on BW following WD. Previous work using heterozygous $Kit^{W\text{-}sh}/Kit^{W\text{-}sh}$ (WBB6F1/J) mice found that these mice were protected from HFD-induced obesity.[38] Our studies potentially diverge from these because we used a different model of MC deficiency (B6.Cg-$Kit^{W\text{-}sh}$/HNihrJaeBsmGlliJ). Another group found that MC depletion using *Mcpt5-Cre R-DTA* mice is not associated with attenuated weight gain and hepatic steatosis following HFD feeding.[39] Again, this is a different model of MC deficiency, and the mice were fed for 21 weeks, which is significantly longer than our 16 weeks of feeding. Lastly, the authors failed to evaluate DR, inflammation, and hepatic fibrosis, which are key features of NAFLD/NASH.

Loss of MCs significantly reduces miR-144-3P levels, and to support this, miR-144-3P expression is significantly increased in patients with NASH versus non-NASH controls.[40] Further, hepatic miR-144-3P levels are increased in obese insulin-resistant humans and mouse models.[41] We propose that miR-144-3P targets ALDH1A3 to promote microvesicular steatosis, which is supported by bioinformatic analyses and luciferase assay. ALDH1A3 is key for clearing toxins and metabolizing aldehydes in cells and can modulate lipid peroxidation.[22] Interestingly, others have found that patients with NASH have decreased hepatic ALDH1A3 levels,[16] which we noted in our mouse model and human NASH samples. Butyrate, a short chain fatty acid, increases ALDH1A3 expression in intestinal epithelial cells[42]; but no other studies have identified ALDH1A3 in steatosis development.

Loss of ALDH1A3 promotes lipid peroxidation,[22] and it has been reported that peroxisome proliferator–activated receptor gamma (PPAR-$\gamma$) suppresses ALDH1A3 expression in lung cancer, which exerts antiproliferative effects through increased lipid peroxidation.[22] We found that WD feeding induced lipid peroxidation, which was further enhanced with MC injections; therefore, we hypothesize that suppressed ALDH1A3 promotes lipid peroxidation during NASH. This hypothesis is relevant considering that lipid peroxidation is key for steatohepatitis development in WD-fed mice,[23,43] and humans with NAFLD have increased lipid peroxidation.[13] Similarly, in mouse models of microvesicular steatosis there is enhanced lipid peroxidation,[19] and it has been reported that MC activation promotes lipid peroxidation in neonatal rat colon.[44]

In conclusion, MCs promote WD-induced steatosis, DR, inflammation, liver fibrosis, and angiogenesis. MC number increases in patients with NAFLD or NASH but more

prominently in NASH, where microvesicular steatosis is noted; therefore, we suggest that MCs promote NAFLD progression to NASH with worsening phenotypes (Fig. 8). Additionally, worsening changes may be mediated by (1) miR-144-3P targeting of ALDH1A3 (promoting microvesicular steatosis) or (2) MC-derived histamine driving biliary senesce, hepatocyte lipogenesis, KC activation, and HSC fibrogenesis. Cromolyn sodium (an MC stabilizer) and over-the-counter HR antagonists (e.g., mepyramine) reduce DR and liver fibrosis in cholestatic models[10,11,21]; therefore, future work is necessary to understand if these therapeutics will benefit patients with NAFLD or NASH. We propose that MC presence indicates worsening phenotypes in NAFLD/NASH, and blocking MC migration or activation may prove therapeutic for this subset of patients.

## Supplementary Material

Refer to Web version on PubMed Central for supplementary material.

## Acknowledgments

Supported by the Hickam Endowed Chair, Gastroenterology, Medicine, Indiana University, and the Indiana University Health–Indiana University School of Medicine Strategic Research Initiative, the SRCS Award, and VA Merit awards (5I01BX000574, to G.A.; 1I01BX003031, to H.F.) from the US Department of Veteran's Affairs, Biomedical Laboratory Research and Development Service, and the National Institutes of Health (DK108959 and DK119421, to H.F.; DK054811, to G.A. and S.G.). This material is the result of work supported by resources at the Central Texas Veterans Health Care System (Temple, TX) and the Richard L. Roudebush VA Medical Center (Indianapolis, IN)

## Abbreviations:

| | |
|---|---|
| **ALDH1A3** | aldehyde dehydrogenase 1 family, member A3 |
| **ALT** | alanine aminotransferase |
| **BDL** | bile duct ligation |
| **BS** | basal |
| **BW** | body weight |
| **CCL** | C-C motif ligand |
| **CD** | control diet |
| **CK-19** | cytokeratin-19 |
| **c-Kit** | KIT proto-oncogene receptor tyrosine kinase |
| **Col1a1** | collagen type 1 α1 |
| **Cpt** | carnitine palmitoyltransferase |
| **DR** | ductular reaction |
| **EIA** | enzyme immunoassay |
| **FFA** | free fatty acid |

| | |
|---|---|
| **H&E** | hematoxylin and eosin |
| **HFD** | high-fat diet |
| **HR** | histamine receptor |
| **HSC** | hepatic stellate cell |
| **IGF-1** | insulin-like growth factor-1 |
| **KC** | Kupffer cell |
| **Kit$^{W\text{-}sh}$** | B6. Cg-Kit$^{W\text{-}sh}$/HNihrJaeBsmJ |
| **LW** | liver weight |
| **m-** | mouse |
| **MC** | mast cell |
| **MDA** | malondialdehyde |
| **miR-144-3p** | microRNA 144–3 prime |
| **miRNA** | microRNA |
| **mMCP-1** | mouse MC protease-1 |
| **NAFLD** | nonalcoholic fatty liver disease |
| **NASH** | nonalcoholic steatohepatitis |
| **PPAR** | peroxisome proliferator–activated receptor |
| **PSC** | primary sclerosing cholangitis |
| **SA-β-Gal** | senescence-associated β-galactosidase |
| **TG** | triglycerides |
| **VEGF-A** | vascular endothelial growth factor-A |
| **WD** | Western diet |
| **WT** | wild type |

## REFERENCES

1. Popescu M, Popescu IA, Stanciu M, Cazacu SM, Ianosi NG, Comanescu MV, et al. Non-alcoholic fatty liver disease—clinical and histopathological aspects. Rom J Morphol Embryol 2016;57:1295–1302 [PubMed: 28174796]
2. Ratziu V, Bonyhay L, Di Martino V, Charlotte F, Cavallaro L, Sayegh-Tainturier M-H, et al. Survival, liver failure, and hepatocellular carcinoma in obesity-related cryptogenic cirrhosis. Hepatology 2002;35:1485–1493. [PubMed: 12029634]
3. Williams CD, Stengel J, Asike MI, Torres DM, Shaw J, Contreras M, et al. Prevalence of nonalcoholic fatty liver disease and nonalcoholic steatohepatitis among a largely middle-

aged population utilizing ultrasound and liver biopsy: a prospective study. Gastroenterology 2011;140:124–131. [PubMed: 20858492]

4. Fromenty B, Pessayre D. Inhibition of mitochondrial beta-oxidation as a mechanism of hepatotoxicity. Pharmacol Ther 1995;67:101–154. [PubMed: 7494860]
5. Tandra S, Yeh MM, Brunt EM, Vuppalanchi R, Cummings OW, Ünalp-Arida A, et al. Presence and significance of microvesicular steatosis in nonalcoholic fatty liver disease. J Hepatol 2011;55:654–659. [PubMed: 21172393]
6. Kennedy L, Hargrove L, Demieville J, Bailey JM, Dar W, Polireddy K, et al. Knockout of l-histidine decarboxylase prevents cholangiocyte damage and hepatic fibrosis in mice subjected to high-fat diet feeding via disrupted histamine/leptin signaling. Am J Pathol 2018;188:600–615. [PubMed: 29248461]
7. Richardson MM, Jonsson JR, Powell EE, Brunt EM, Neuschwander–Tetri BA, Bhathal PS, et al. Progressive fibrosis in nonalcoholic steatohepatitis: association with altered regeneration and a ductular reaction. Gastroenterology 2007;133:80–90. [PubMed: 17631134]
8. Beaven MA. Our perception of the mast cell from Paul Ehrlich to now. Eur J Immunol 2009;39:11–25. [PubMed: 19130582]
9. Hargrove L, Kennedy L, Demieville J, Jones H, Meng F, DeMorrow S, et al. Bile duct ligation–induced biliary hyperplasia, hepatic injury, and fibrosis are reduced in mast cell-deficient $Kit^{W\text{-}sh}$ mice. HEPATOLOGY 2017;65:1991–2004 [PubMed: 28120369]
10. Kennedy L, Hargrove L, Demieville J, Karstens W, Jones H, DeMorrow S, et al. Blocking H1/H2 histamine receptors inhibits damage/fibrosis in $Mdr2^{-/-}$ mice and human cholangiocarcinoma tumorigenesis. Hepatology 2018;68:1042–1056. [PubMed: 29601088]
11. Kennedy LL, Hargrove LA, Graf AB, Francis TC, Hodges KM, Nguyen QP, et al. Inhibition of mast cell–derived histamine secretion by cromolyn sodium treatment decreases biliary hyperplasia in cholestatic rodents. Lab Invest 2014;94:1406–1418. [PubMed: 25365204]
12. Hargrove L, Graf-Eaton A, Kennedy L, Demieville J, Owens J, Hodges K, et al. Isolation and characterization of hepatic mast cells from cholestatic rats. Lab Invest 2016;96:1198–1210. [PubMed: 27548803]
13. Konishi M, Iwasa M, Araki J, Kobayashi Y, Katsuki A, Sumida Y, et al. Increased lipid peroxidation in patients with nonalcoholic fatty liver disease and chronic hepatitis C as measured by the plasma level of 8-isoprostane. J Gastroenterol Hepatol 2006;21:1821–1825. [PubMed: 17074020]
14. Hsu LC, Chang WC, Hiraoka L, Hsieh CL. Molecular cloning, genomic organization, and chromosomal localization of an additional human aldehyde dehydrogenase gene, ALDH6. Genomics 1994;24:333–341. [PubMed: 7698756]
15. Yin H, Xu L, Porter NA. Free radical lipid peroxidation: mechanisms and analysis. Chem Rev 2011;111:5944–5972. [PubMed: 21861450]
16. Pettinelli P, Arendt BM, Teterina A, McGilvray I, Comelli EM, Fung SK, et al. Altered hepatic genes related to retinol metabolism and plasma retinol in patients with non-alcoholic fatty liver disease. PLoS One 2018;13:e0205747. [PubMed: 30379862]
17. Macdonald GA, Bridle KR, Ward PJ, Walker NI, Houglum K, George DK, et al. Lipid peroxidation in hepatic steatosis in humans is associated with hepatic fibrosis and occurs predominately in acinar zone 3. J Gastroenterol Hepatol 2001;16:599–606. [PubMed: 11422610]
18. Fromenty B, Berson A, Pessayre D. Microvesicular steatosis and steatohepatitis: role of mitochondrial dysfunction and lipid peroxidation. J Hepatol 1997;26(Suppl. 1):13–22. [PubMed: 9138124]
19. Natarajan SK, Eapen CE, Pullimood AB, Balasubramanian KA. Oxidative stress in experimental liver microvesicular steatosis: role of mitochondria and peroxisomes. J Gastroenterol Hepatol 2006;21:1240–1249. [PubMed: 16872304]
20. Lessmann E, Grochowy G, Weingarten L, Giesemann T, Aktories K, Leitges M, et al. Insulin and insulin-like growth factor-1 promote mast cell survival via activation of the phosphatidylinositol3-kinase pathway. Exp Hematol 2006;34:1532–1541. [PubMed: 17046573]

21. Jones H, Hargrove L, Kennedy L, Meng F, Graf-Eaton A, Owens J, et al. Inhibition of mast cell–secreted histamine decreases biliary proliferation and fibrosis in primary sclerosing cholangitis Mdr2$^{-/-}$ mice. Hepatology 2016;64:1202–1216. [PubMed: 27351144]
22. Hua TNM, Namkung J, Phan ANH, Vo VTA, Kim MK, Jeong Y, et al. PPARgamma-mediated ALDH1A3 suppression exerts antiproliferative effects in lung cancer by inducing lipid peroxidation. J Recept Signal Transduct Res 2018;38:191–197. [PubMed: 29873276]
23. Morita M, Ishida N, Uchiyama K, Yamaguchi K, Itoh Y, Shichiri M, et al. Fatty liver induced by free radicals and lipid peroxidation. Free Radic Res 2012;46:758–765. [PubMed: 22468959]
24. Nobili V, Carpino G, Alisi A, Franchitto A, Alpini G, De Vito R, et al. Hepatic progenitor cells activation, fibrosis, and adipokines production in pediatric nonalcoholic fatty liver disease. Hepatology 2012;56:2142–2153. [PubMed: 22467277]
25. Johnson C, Huynh V, Hargrove L, Kennedy L, Graf-Eaton A, Owens J, et al. Inhibition of mast cell–derived histamine decreases human cholangiocarcinoma growth and differentiation via c-Kit/stem cell factor-dependent signaling. Am J Pathol 2016;186:123–133. [PubMed: 26597881]
26. Lombardo J, Broadwater D, Collins R, Cebe K, Brady R, Harrison S. Hepatic mast cell concentration directly correlates to stage of fibrosis in NASH. Hum Pathol 2019;86:129–135. [PubMed: 30597154]
27. Yamashiro M, Kouda W, Kono N, Tsuneyama K, Matsui O, Nakanuma Y. Distribution of intrahepatic mast cells in various hepatobiliary disorders. An immunohistochemical study. Virchows Arch 1998;433:471–479. [PubMed: 9849863]
28. Smith DD, Tan X, Raveendran VV, Tawfik O, Stechschulte DJ, Dileepan KN. Mast cell deficiency attenuates progression of atherosclerosis and hepatic steatosis in apolipoprotein E-null mice. Am J Physiol Heart Circ Physiol 2012;302:H2612–H2621. [PubMed: 22505639]
29. Coulon S, Francque S, Colle I, Verrijken AN, Blomme B, Heindryckx F, et al. Evaluation of inflammatory and angiogenic factors in patients with non-alcoholic fatty liver disease. Cytokine 2012;59:442–449. [PubMed: 22658783]
30. Yokoyama M, Yokoyama A, Mori S, Takahashi HK, Yoshino T, Watanabe T, et al. Inducible histamine protects mice from *P. acnes*-primed and LPS-induced hepatitis through H2-receptor stimulation. Gastroenterology 2004;127:892–902. [PubMed: 15362044]
31. Ahmad SF, Ansari MA, Zoheir KM, Bakheet SA, Korashy HM, Nadeem A, et al. Regulation of TNF-alpha and NF-kappaB activation through the JAK/STAT signaling pathway downstream of histamine 4 receptor in a rat model of LPS-induced joint inflammation. Immunobiology 2015;220:889–898. [PubMed: 25666529]
32. Kennedy L, Meadows V, Demieville J, Hargrove L, Virani S, Glaser S, et al. Biliary damage and liver fibrosis are ameliorated in a novel mouse model lacking l-histidine decarboxylase/histamine signaling. Lab Invest 2020;100:837–848. [PubMed: 32054995]
33. Tashiro K, Takai S, Jin D, Yamamoto H, Komeda K, Hayashi M, et al. Chymase inhibitor prevents the nonalcoholic steatohepatitis in hamsters fed a methionine- and choline-deficient diet. Hepatol Res 2010;40:514–523. [PubMed: 20374300]
34. Ciupinska-Kajor M, Hartleb M, Kajor M, Kukla M, Wylezol M, Lange D, et al. Hepatic angiogenesis and fibrosis are common features in morbidly obese patients. Hepatol Int 2013;7:233–240. [PubMed: 23519653]
35. Wu N, Meng F, Zhou T, Han Y, Kennedy L, Venter J, et al. Prolonged darkness reduces liver fibrosis in a mouse model of primary sclerosing cholangitis by miR-200b down-regulation. FASEB J 2017;31:4305–4324. [PubMed: 28634212]
36. Ferri F, Lai Q, Molinaro A, Poli E, Parlati L, Lattanzi B, et al. Donor small-droplet macrovesicular steatosis affects liver transplant outcome in HCV-negative recipients. Can J Gastroenterol Hepatol 2019;2019:5862985. [PubMed: 31187028]
37. Franceschini B, Russo C, Dioguardi N, Grizzi F. Increased liver mast cell recruitment in patients with chronic C virus–related hepatitis and histologically documented steatosis. J Viral Hepat 2007;14:549–555. [PubMed: 17650288]
38. Liu J, Divoux A, Sun J, Zhang J, Clément K, Glickman JN, et al. Genetic deficiency and pharmacological stabilization of mast cells reduce diet-induced obesity and diabetes in mice. Nat Med 2009;15:940–945. [PubMed: 19633655]

39. Chmelar J, Chatzigeorgiou A, Chung KJ, Prucnal M, Voehringer D, Roers A, et al. No role for mast cells in obesity-related metabolic dysregulation. Front Immunol 2016;7:524. [PubMed: 27933062]

40. Vega-Badillo J, Gutierrez-Vidal R, Hernandez-Perez HA, Villamil-Ramirez H, Leon-Mimila P, Sanchez-Munoz F, et al. Hepatic miR-33a/miR-144 and their target gene ABCA1 are associated with steatohepatitis in morbidly obese subjects. Liver Int 2016;36:1383–1391. [PubMed: 26945479]

41. Azzimato V, Jager J, Chen P, Morgantini C, Levi L, Barreby E, et al. Liver macrophages inhibit the endogenous antioxidant response in obesity-associated insulin resistance. Sci Transl Med 2020;12:eaaw9709. [PubMed: 32102936]

42. Schilderink R, Verseijden C, Seppen J, Muncan V, van den Brink GR, Lambers TT, et al. The SCFA butyrate stimulates the epithelial production of retinoic acid via inhibition of epithelial HDAC. Am J Physiol Gastrointest Liver Physiol 2016;310:G11 38–G1146.

43. Letteron P, Fromenty B, Terris B, Degott C, Pessayre D. Acute and chronic hepatic steatosis lead to in vivo lipid peroxidation in mice. J Hepatol 1996;24:200–208. [PubMed: 8907574]

44. Brown JF, Chafee KA, Tepperman BL. Role of mast cells, neutrophils and nitric oxide in endotoxin-induced damage to the neonatal rat colon. Br J Pharmacol 1998;123:31–38. [PubMed: 9484851]

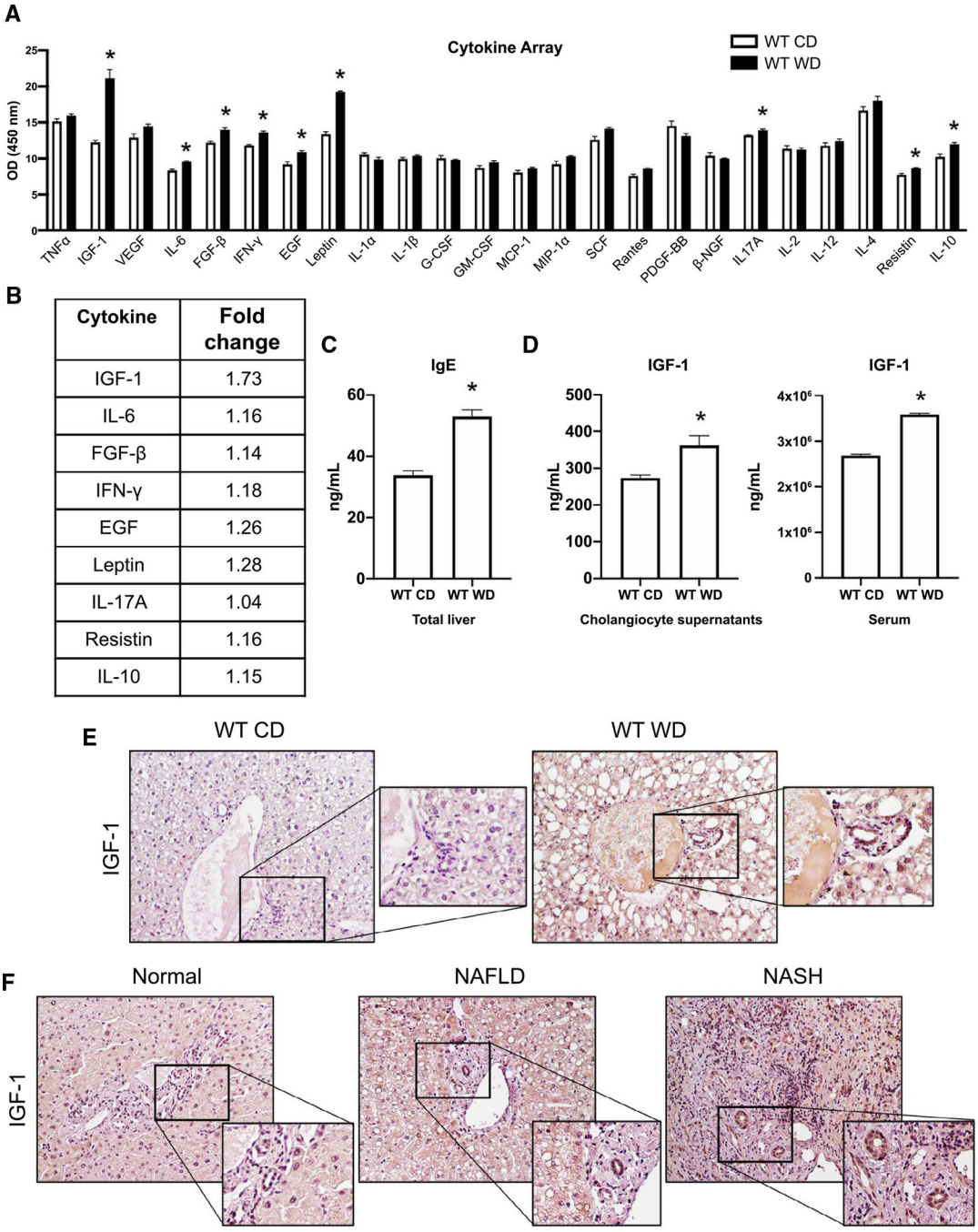


| Cytokine | Fold change |
|---|---|
| IGF-1 | 1.73 |
| IL-6 | 1.16 |
| FGF-β | 1.14 |
| IFN-γ | 1.18 |
| EGF | 1.26 |
| Leptin | 1.28 |
| IL-17A | 1.04 |
| Resistin | 1.16 |
| IL-10 | 1.15 |

**FIG. 1.**

Biliary IGF-1 secretion and expression. (A) Cytokine multiELISA showed increased release of IGF-1, IL-6, FGF-β, IFN-γ, EGF, leptin, IL-17A, resistin, and IL-10 in WT WD mice compared to WT CD mice. (B) Fold change of the increased cytokines. (C) IgE levels in liver lysates increased in WT WD mice compared to WT CD mice. (D) IGF-1 secretion is increased in cholangiocyte supernatants and serum from WT WD mice compared to WT CD mice. (E) IGF-1 immunoreactivity is enhanced in WT WD mice compared to WT CD mice. (F) IGF-1 immunoreactivity is enhanced in human NASH compared to normal. n =

3 reactions from n = 10–15 mice for multiELISA, n = 4 reactions from n = 4 mice for IgE ELISA, n = 4 reactions from n = 8–10 mice for IGF-1 enzyme immunoassay (EIA). Data are mean ± SEM. *$P < 0.05$ versus WT CD mice. IGF-1 immunostaining shown at ×20 and ×60. Abbreviations: G-CSF, granulocyte colony-stimulating factor; GM-CSF, granulocyte-macrophage colony-stimulating factor; IFN-γ, interferon gamma; MIP-1α, macrophage inflammatory protein 1 alpha; NGF, nerve growth factor; OD, optical density; PDGF, platelet-derived growth factor; RANTES, regulated upon activation, normal T cell expressed, and secreted; SCF, stem cell factor.

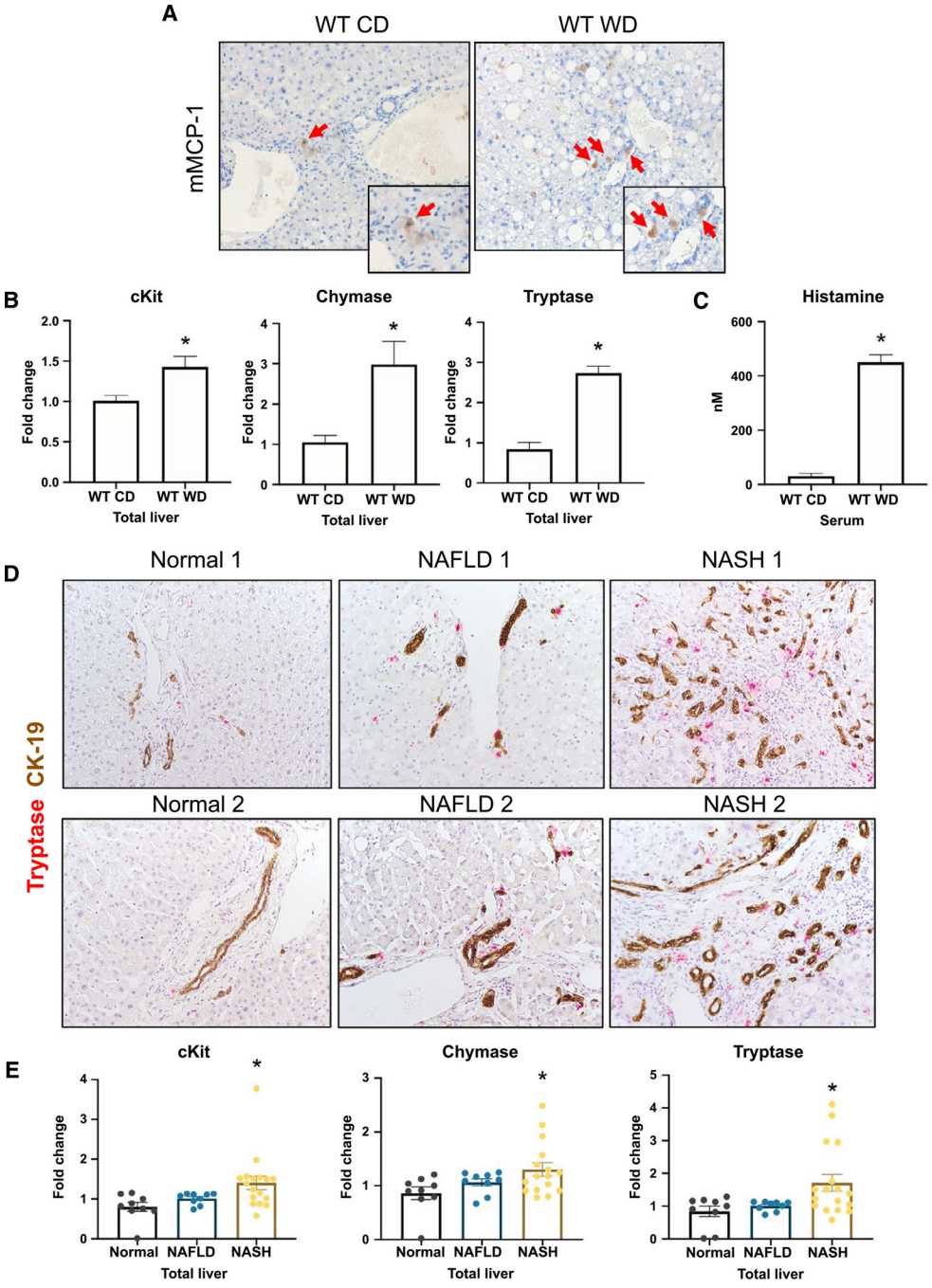


**FIG. 2.**

MC presence and activation. WT WD mice had increased (A) mMCP-1 (MC marker, red arrows) expression; (B) chymase, tryptase, and c-Kit mRNA expression; and (C) serum histamine levels. (D) MCs (tryptase) and DR (CK-19) increased in patients with NAFLD or NASH. (E) Chymase, tryptase, and c-Kit mRNA expression increased in human NASH. n = 4 reactions from n = 10–15 mice for quantitative PCR; n = 2–4 reactions per sample from n = 9 normal, n = 9 NAFLD, and n = 17 NASH human samples for quantitative PCR; n = 4 reactions from n = 10–15 mice for EIA. Data are mean ± SEM. **P* < 0.05 versus WT CD

mice or human normal. mMCP-1 immunostaining shown at ×20 and ×40, tryptase/CK-19 coimmunostaining shown at ×20.

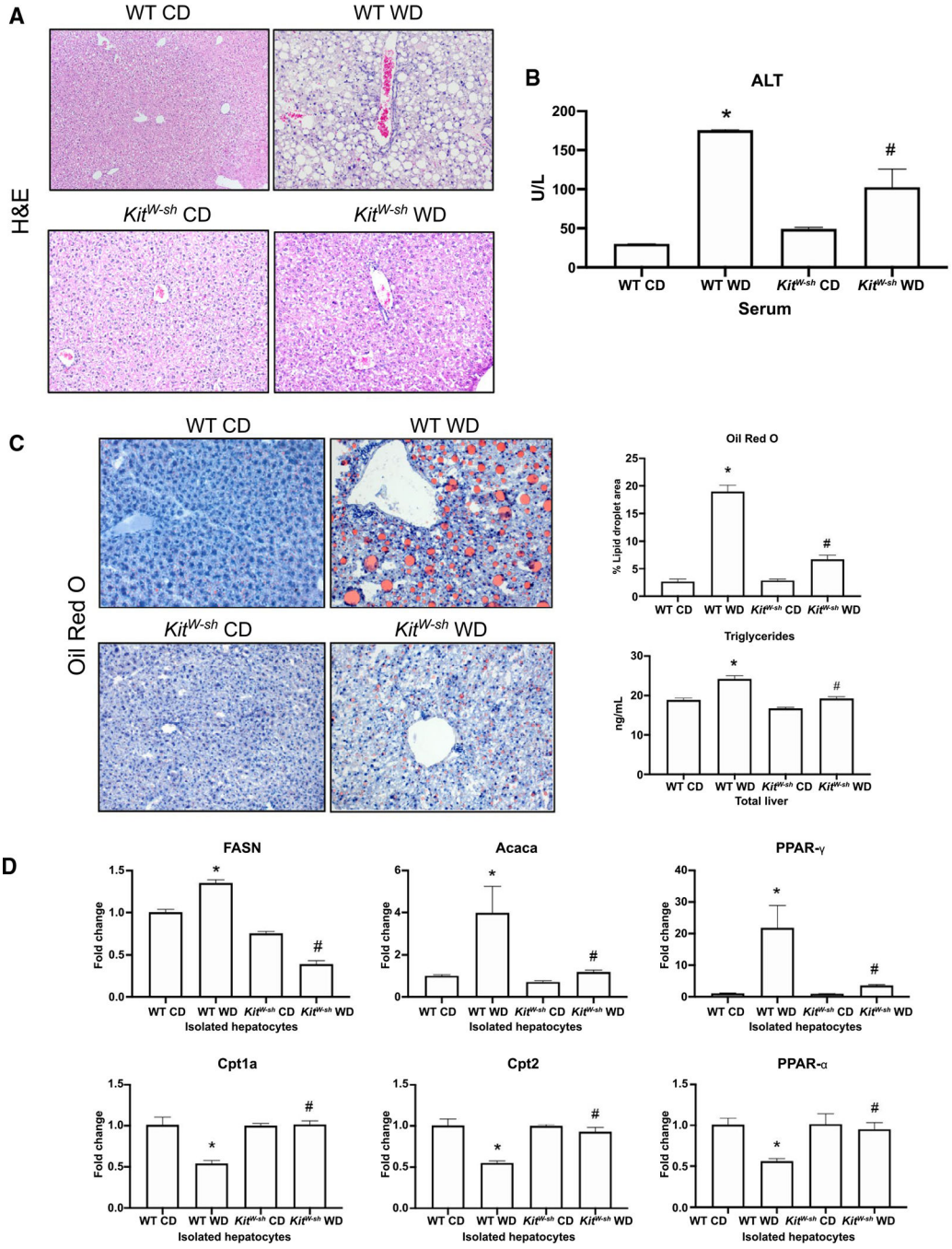


**FIG. 3.**

Liver steatosis and hepatocyte lipogenesis. (A) H&E showed increased steatosis, inflammation, and DR in WT WD mice, which was reduced in *Kit*$^{W\text{-}sh}$ WD mice. (B) Serum ALT increased in WT WD mice compared to WT CD mice but decreased in *Kit*$^{W\text{-}sh}$ WD mice compared to WT WD mice. (C) By oil red O staining, percentage lipid droplet area increased in WT WD mice, which was reduced in *Kit*$^{W\text{-}sh}$ WD mice. Similar findings were noted for hepatic TG content. (D) Lipogenesis markers FASN, Acaca, and PPAR-γ were increased in hepatocytes from WT WD mice compared to WT CD mice but reduced

in $Kit^{W\text{-}sh}$ WD mice compared to WT WD mice. mRNA expression of β-oxidation markers carnitine palmitoyltransferase 1a (Cpt1a), Cpt2, and PPAR-α decreased in hepatocytes from WT WD mice compared to WT CD mice but increased in $Kit^{W\text{-}sh}$ WD mice compared to WT WD mice. n = 4 reactions from n = 8–15 mice for ALT, n = 10 images from n = 8–15 mice for oil red O, n = 4 reactions from n = 8–15 mice for TG EIA, n = 4 reactions from n = 8–15 mice for quantitative PCR. Data are mean ± SEM. $^{*}P < 0.05$ versus WT CD mice; $^{\#}P < 0.05$ versus WT WD mice. H&E shown at ×10, oil red O shown at ×20. Abbreviations: Acaca, acetyl-CoA carboxylase 1; FASN, fatty acid synthase.

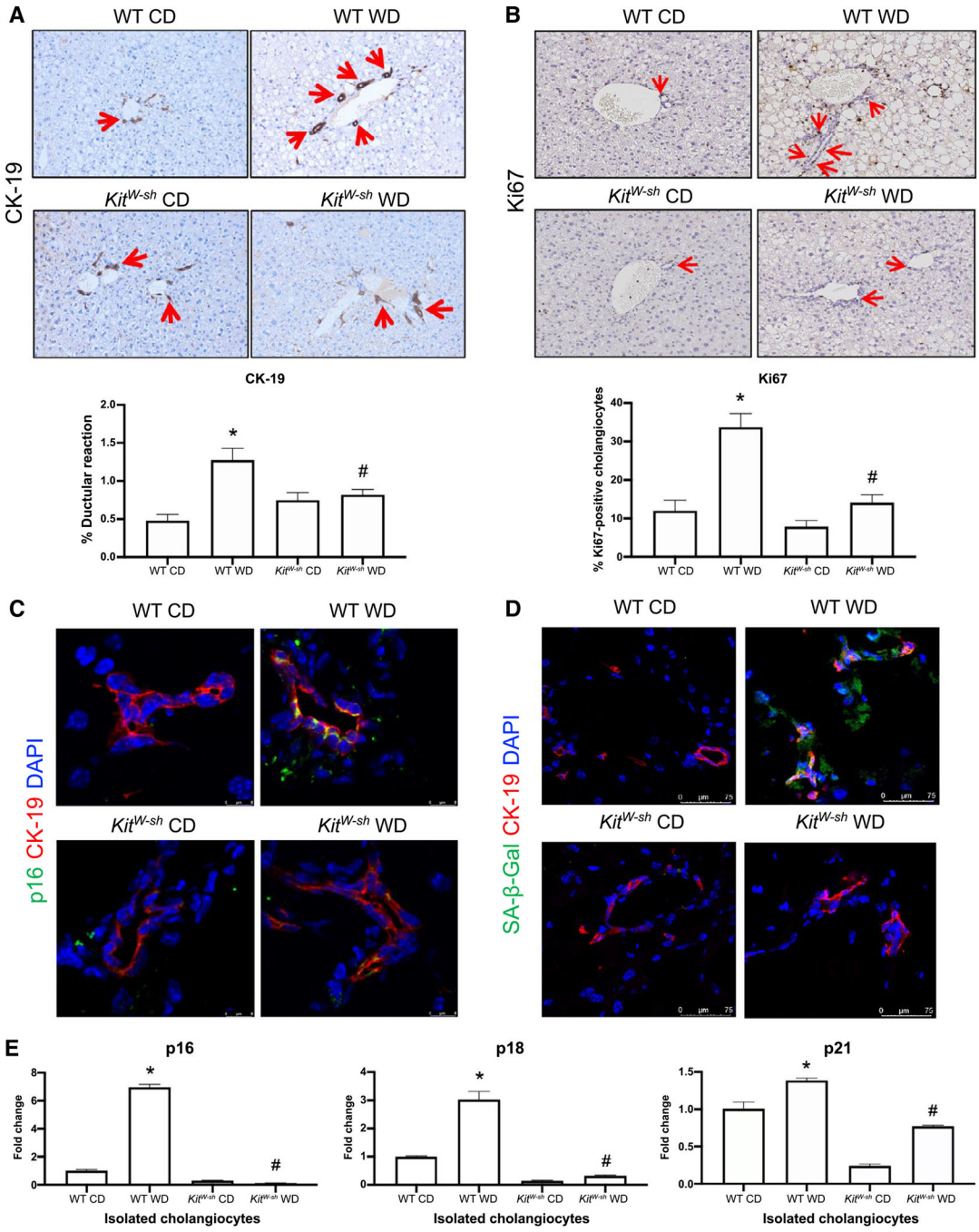


**FIG. 4.**

DR and biliary senescence. Immunostaining for (A) CK-19 and (B) Ki67 indicated increased DR and biliary proliferation (red arrows) in WT WD mice compared to WT CD mice, which decreased in *Kit*$^{W\text{-}sh}$ WD mice compared to WT WD mice. Immunofluorescence for (C) p16 and (D) SA-β-Gal (both costained with CK-19) showed enhanced biliary senescence in WT WD mice compared to WT CD mice, which decreased in *Kit*$^{W\text{-}sh}$ WD mice compared to WT WD mice. (E) Expression of senescence markers increased in isolated cholangiocytes from WT WD mice compared to WT CD mice but decreased in *Kit*$^{W\text{-}sh}$ WD mice compared

to WT WD mice. n = 10 images from n = 8 mice for CK-19 and Ki67, n = 4 reactions from n = 8–15 mice for quantitative PCR. Data are mean ± SEM. *$P < 0.05$ versus WT CD mice; #$P < 0.05$ versus WT WD mice. CK-19 and Ki67 staining shown at ×20, p16/CK-19 staining shown at ×160, SA-β-Gal/CK-19 staining shown at ×80.

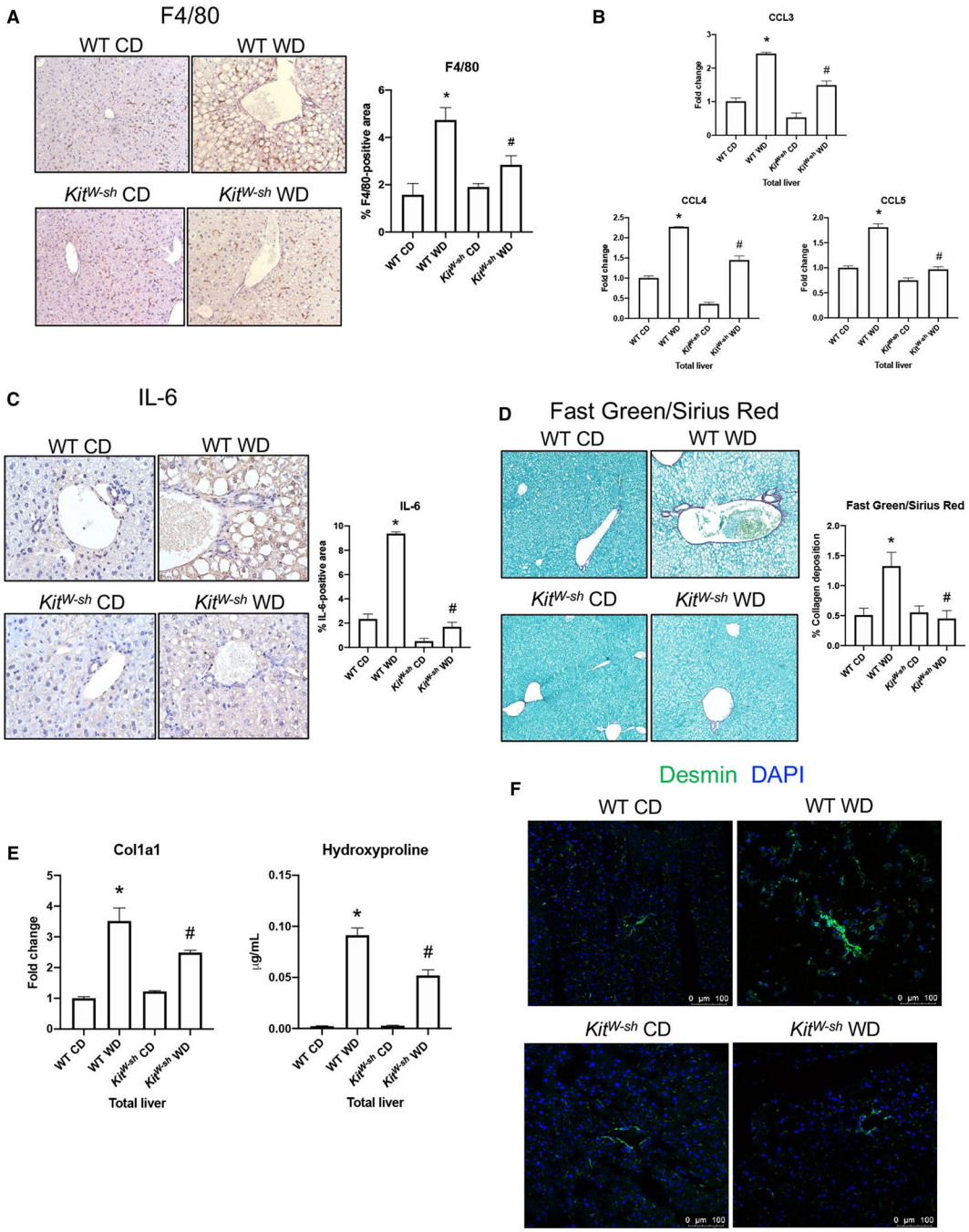


**FIG. 5.**

KC presence, liver inflammation, and liver fibrosis. WT WD mice had increased (A) KC presence; (B) CCL3, CCL4, and CCL5 mRNA expression; and (C) IL-6 expression compared to WT CD mice, which decreased in *Kit*$^{W\text{-}sh}$ WD mice. WT WD mice had increased (D) collagen deposition (fast green/sirius red); (E) Col1a1 mRNA expression and hydroxyproline levels; and (F) desmin expression (HSC marker) compared with WT CD mice; but these parameters were decreased in *Kit*$^{W\text{-}sh}$ WD mice compared to WT WD mice. n = 4 reactions from n = 8–10 mice for quantitative PCR, n = 10 images from n = 8–10 mice

for staining, n = 6 reactions from n = 8–10 mice for hydroxyproline assay. Data are mean ± SEM. *$P < 0.05$ versus WT CD mice; $^{\#}P < 0.05$ versus WT WD mice. Immunostaining shown at ×10 for F4/80 and ×20 for IL-6, sirius red/fast green shown at ×10, desmin staining shown at ×20.

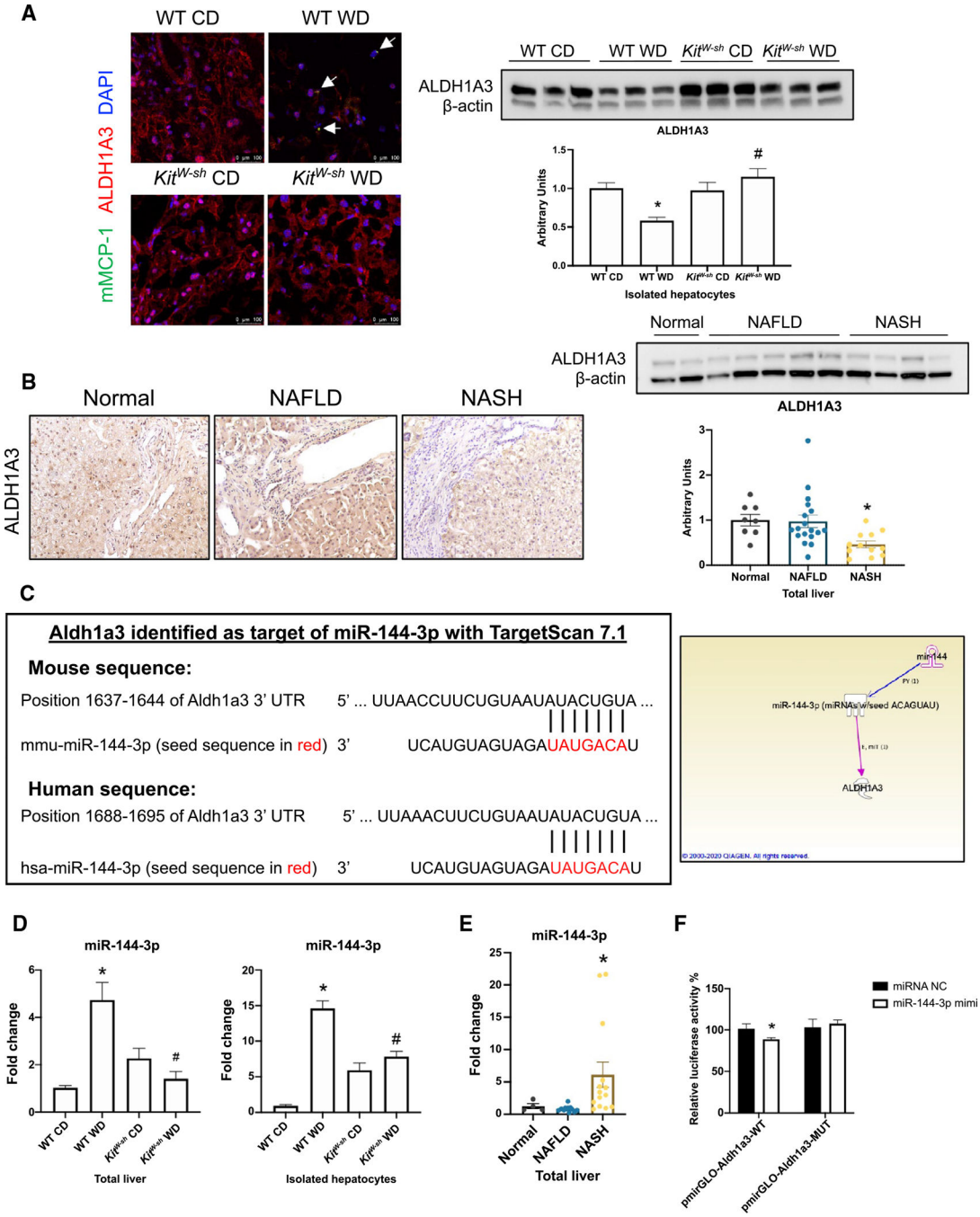


**FIG. 6.**

miR-144-3p/ALDH1A3 signaling mechanism. (A) ALDH1A3 expression is reduced in WT WD mice, concomitant with increased MC presence (white arrows), compared to WT CD mice; but this is reversed in *Kit*$^{W\text{-}sh}$ WD mice compared to WT WD mice, as indicated by immunostaining and western blotting. (B) ALDH1A3 expression is unchanged in human NAFLD compared to normal but reduced in human NASH, as determined by immunostaining and western blotting. (C) TargetScan software identified miR-144-3p as a highly conserved miRNA targeting ALDH1A3, and miR-144-3p targeting of ALDH1A3

was confirmed by IPA. (D) miR-144-3P expression is increased in total liver and isolated hepatocytes from WT WD mice compared to WT CD mice but decreased in $Kit^{W\text{-}sh}$ WD mice compared to WT WD mice. (E) Similarly, miR-144-3P expression is increased in human NASH compared to normal; there is no change between NAFLD and normal. (F) By luciferase assay, miR-144-3P significantly decreases Aldh1a3-WT expression, but this down-regulation is ablated by the Aldh1a3 mutant form. n = 6 bands from n = 10–15 mice for western blotting, n = 1 band per sample from n = 4 normal, n = 9 NAFLD and n = 7 NASH total liver samples for western blotting, n = 9–12 reactions for total liver and n = 3 reactions for isolated hepatocytes from n = 10–15 mice for quantitative PCR, n = 3 reactions per sample from n = 4 normal, n = 12 NAFLD and n = 14 NASH for human total liver quantitative PCR, n = 5 reactions for luciferase assay. Data are mean ± SEM. $^{*}P < 0.05$ versus WT CD mice, miRNA normal control, or normal human patient; $^{\#}P < 0.05$ versus WT WD mice. Mouse staining shown at ×80, and human staining shown at ×40. Abbreviations: NC, normal control; UTR, untranslated region.

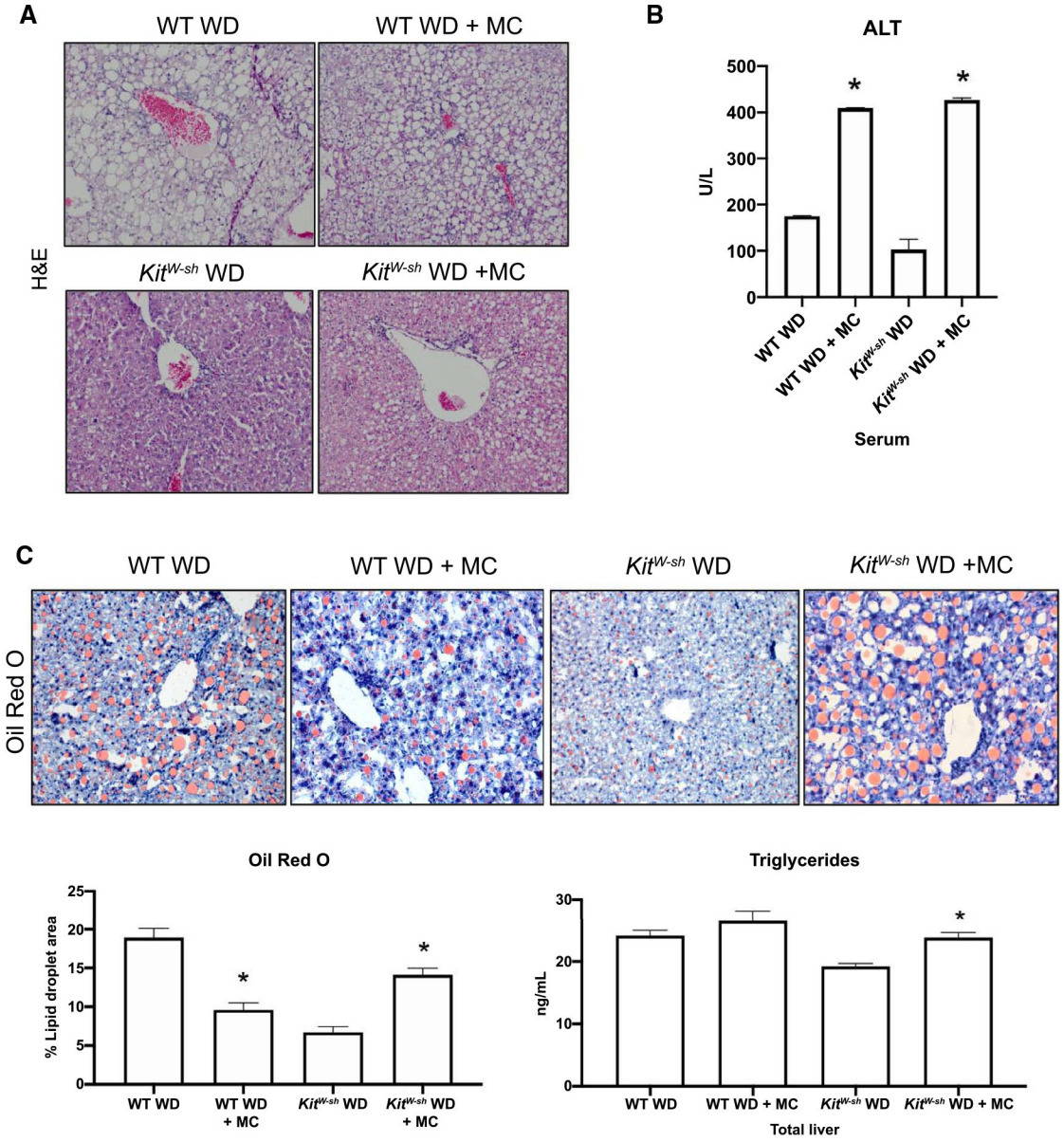


**FIG. 7.**

Changes in liver damage and steatosis following MC injections. (A) Microvesicular steatosis, inflammation, and DR increased in WT WD+MC mice compared to WT WD mice. *Kit*$^{W\text{-}sh}$ WD+MC mice had increased microvesicular steatosis, inflammation, and DR compared to *Kit*$^{W\text{-}sh}$ WD mice. (B) Serum levels of ALT are significantly increased in WT WD and *Kit*$^{W\text{-}sh}$ WD mice following MC injections compared to controls. (C) Oil red O staining showed a reduction in lipid droplet area (indicative of microvesicular steatosis development) in WT WD+MC mice compared to WT WD mice; however, *Kit*$^{W\text{-}sh}$ WD+MC mice had an increase in lipid droplet area compared to *Kit*$^{W\text{-}sh}$ WD mice. Hepatic TGs are unchanged in WT WD+MC mice compared to WT WD mice but increased in *Kit*$^{W\text{-}sh}$ WD+MC mice compared to *Kit*$^{W\text{-}sh}$ WD mice. n = 5 reactions for serum chemistry from n = 10–13 mice, n = 10 images from n = 10–13 mice for oil red O staining, n = 4 reactions

from n = 10–13 mice for TG EIA. Data are mean ± SEM. *$P < 0.05$ versus WT WD mice or $Kit^{W\text{-}sh}$ WD mice. H&E staining shown at ×10, oil red O staining shown at ×20.

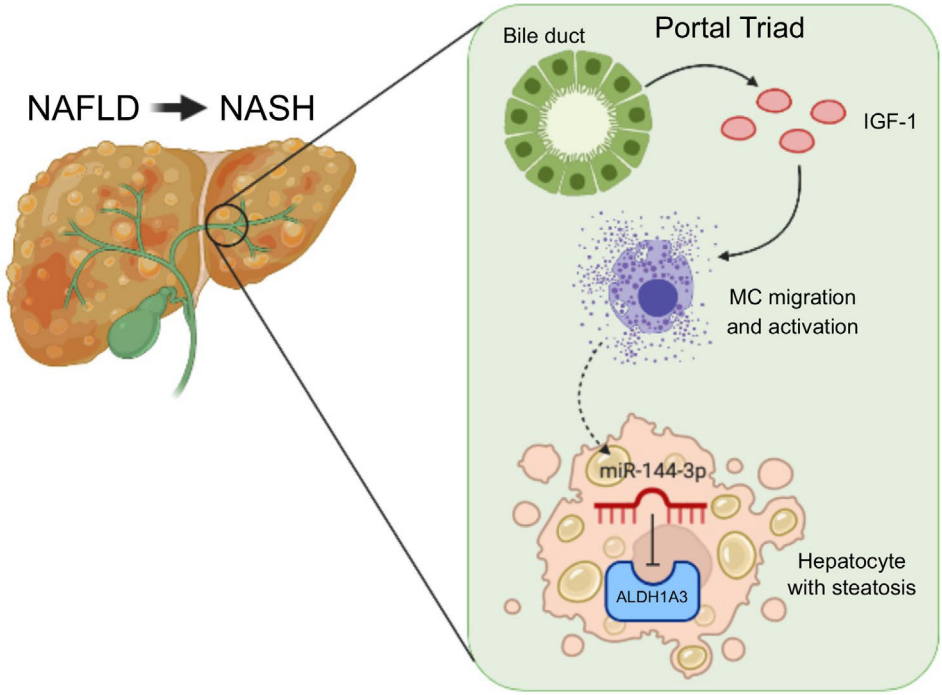


**FIG. 8.**

Working model. During NAFLD progression to NASH, bile ducts are injured and increase secretion of IGF-1, which promotes MC migration to the portal areas. Enhanced MC migration and activation increase miR-144-3P expression in hepatocytes, which inhibits and down-regulates ALDH1A3 expression. Image made with Bio Render.